

Learning Test-time Augmentation for Content-based Image Retrieval

Osman Tursun^{a,**}, Simon Denman^a, Sridha Sridharan^a, Clinton Fookes^a

^aSignal Processing, Artificial Intelligence and Vision Technologies (SAIVT), Queensland University of Technology, Australia

ABSTRACT

Off-the-shelf convolutional neural network features achieve outstanding results in many image retrieval tasks. However, their invariance to target data is pre-defined by the network architecture and training data. Existing image retrieval approaches require fine-tuning or modification of pre-trained networks to adapt to variations unique to the target data. In contrast, our method enhances the invariance of off-the-shelf features by aggregating features extracted from images augmented at test-time, with augmentations guided by a policy learned through reinforcement learning. The learned policy assigns different magnitudes and weights to the selected transformations, which are selected from a list of image transformations. Policies are evaluated using a metric learning protocol to learn the optimal policy. The model converges quickly and the cost of each policy iteration is minimal as we propose an off-line caching technique to greatly reduce the computational cost of extracting features from augmented images. Experimental results on large trademark retrieval (METU trademark dataset) and landmark retrieval (ROxford5k and RParis6k scene datasets) tasks show that the learned ensemble of transformations is highly effective for improving performance, and is practical, and transferable.

1. Introduction

The internal activations of convolutional neural networks (CNNs) pre-trained on ImageNet have demonstrated astounding results when utilised for various object (image) retrieval tasks Sharif Razavian et al. (2014); Tursun et al. (2019). Such activations are termed off-the-shelf CNN features and compared to conventional hand-crafted features, they are more discriminative, compact and accessible. To this end, off-the-shelf CNN features are widely used for object retrieval over or in combination with conventional hand-crafted features.

However, un-altered off-the-shelf features are often not sufficiently robust to adapt to variations in the target data including changes in scale, illumination, orientation, color, contrast, deformations, and background clutter Aker et al. (2017); Gong et al. (2014). Thus image retrieval using such features can fail when these challenges are present in test data, as un-altered off-the-shelf features have no in-built invariances beyond translational invariance. This is due to these networks being predominantly trained with natural images and light data augmentation.

For example, ResNet He et al. (2015) was trained with only the simple data augmentations of random-crops and horizontal flips. Therefore, off-the-shelf features are not scale, rotation or contrast invariant. However, transform invariant features are desirable for challenging object retrieval tasks.

Many methods have been proposed to enhance the transform invariance of CNN features for classification and recognition. Those methods incorporate transform invariance either via special network structures, data augmentation, or both. Feature extraction modules (*i.e.*, spatial transformer Jaderberg et al. (2015), transform capsules Hinton et al. (2011), multi-column networks Ciregan et al. (2012)) and alternate filter formulations (*i.e.*, deformable filters Dai et al. (2017), transformed filters Marcos et al. (2016); Follmann and Bottger (2018) and pooling Gong et al. (2014); Marcos et al. (2016); Tolias et al. (2015)) are types of neural structure that can improve the transform invariance of neural networks. Generally, these models require training, or are only valid for certain datasets or transformations (*i.e.*, scale or rotation), and so lack generality. By comparison, data augmentation is a simple but effective way to achieve transform invariance as only extra transformations on input images are necessary during training or inference. This allows the generation of a more robust descriptor from multiple transformed samples, and the cost of data augmentation can be minimised

^{**}Corresponding author
e-mail: osman.tursun@qut.edu.au (Osman Tursun)

by parallelization.

In this work, we propose an automatic test-time augmentation (auto TTA) that uses an ensemble of learned test-time augmentations (TTA) applied to a single input image to increase the invariance of off-the-shelf features, without sacrificing their compactness and discriminability. Our key motivation is to improve the performance off-the-shelf-features for image retrieval without network fine-tuning. Approaches that fine-tune off-the-shelf features are computationally expensive, noise-sensitive and face the risk of over-fitting and losing generality. Moreover, fine-tuning is only effective for the data on which the model is fine-tuned, and does not increase the generality of the underlying model. Existing fine-tuning-free studies for image retrieval are related to pooling [Gong et al. \(2014\)](#); [Marcos et al. \(2016\)](#); [Tolias et al. \(2015\)](#), feature selection/aggregation [Gong et al. \(2014\)](#) or hand-crafted TTA (*i.e.*, scaling, rotating). Compared to hand-crafted TTA, our approach exploits other data augmentations besides scaling and rotating, and requires no expert knowledge of the target image retrieval task. Additionally, the proposed auto TTA method not only learns transformations and their magnitudes, but also assigns weights to each transformation. In comparison, traditional hand-crafted TTA approaches such as multi-scale resizing only utilise a single type of transformation with pre-selected magnitudes and uniform weights.

We propose a simple but effective and efficient procedure for automating the learning process of the optimal TTA for image retrieval. Finding the optimal ensemble of TTA is a discrete search problem. Random, grid and heuristic searches are possible solutions but are expensive and impractical. Reinforcement learning-based searching has been widely used for discrete search problems [Zoph and Le \(2016\)](#); [Cubuk et al. \(2019\)](#) such as neural architecture search (NAS) [Zoph and Le \(2016\)](#). We therefore apply a reinforcement learning-based search to find the best ensemble of TTA to extract invariant features for image retrieval. Usually, neural hyper-parameter search and NAS with reinforcement learning require enormous computational resources and are time-consuming. For example, learning data augmentations with NAS requires at least 5,000/15,000 GPU hours on the CIFAR10/ImageNet datasets as reported by [Cubuk et al. \(2019\)](#). We reduce this time complexity to less than 4 GPU hours with the following improvements:

- Reducing the time cost of each learning iteration. We avoid the repeated deep feature extraction process by reusing transformed features through off-line feature caching.
- Improving the rate of convergence during training. To this end, we proposed a metric-learning (triplet loss) based framework where a list of image transformations with customized settings and transformations for image retrieval tasks are utilised.

With this framework, the training starts to converge after approximately 2000 steps.

Our experimental results on trademark (METU trademark [Tursun et al. \(2017\)](#) dataset) and landmark retrieval (ROxford5k [Philbin et al. \(2007\)](#); [Radenović et al. \(2018\)](#) and RParis6k [Philbin et al. \(2008\)](#); [Radenović et al. \(2018\)](#) datasets) tasks

show the learned ensemble of image transformations increases the performance of off-the-shelf features. The learned transformation demonstrates its transferability to off-the-shelf features from different pre-trained networks, and is applicable to various aggregation methods. We achieve SOTA comparable MAP results on the challenging METU trademark dataset with the learned ensemble of TTA.

In summary, our contribution in this paper is threefold:

- We propose a new approach, learned TTA, for boosting off-the-shelf deep features performance on content-based image retrieval (CBIR) task by learning a weighted combination of augmentations.
- To make this approach efficient and effective, we introduce metric-learning based training framework, off-line feature caching and a list of customised image transformations.
- Experimental results on trademark retrieval and landmark retrieval tasks show that the learned TTA is highly effective for improving performance, and is practical and transferable.

2. Related Literature

In this section, we introduce recent studies on test time augmentation (TTA) and content-based image retrieval (CBIR) with deep features.

2.1. Test Time Augmentation

Test-time augmentation has been widely used for image recognition and retrieval tasks [Gong et al. \(2014\)](#); [Krizhevsky et al. \(2012\)](#); [Simonyan and Zisserman \(2014\)](#); [Szegedy et al. \(2015\)](#) due to its effectiveness. Multi-cropping and horizontal-flipping are applied when using AlexNet [Krizhevsky et al. \(2012\)](#), VGG16 [Simonyan and Zisserman \(2014\)](#), ResNet [He et al. \(2015\)](#), and Inception [Szegedy et al. \(2015\)](#) models. Multi-scale cropping is introduced by [Gong et al. \(2014\)](#), and brings improvements for both image recognition and retrieval tasks. Scaling (high resolution inputs) improves performance in image retrieval tasks [Babenko and Lempitsky \(2015\)](#); [Radenović et al. \(2018\)](#) where results with inputs at a resolution of 1,024 square are better than results with images at lower resolutions such as 512 or 256 square. Other types of data augmentation techniques such as rotation [Perez et al. \(2018\)](#); [Matsunaga et al. \(2017\)](#); [Wang et al. \(2018\)](#), translation [Perez et al. \(2018\)](#); [Matsunaga et al. \(2017\)](#); [Wang et al. \(2018\)](#), color shifting [Perez et al. \(2018\)](#); [Nalepa et al. \(2019\)](#) and random noise [Wang et al. \(2018\)](#) are also used at test-time for recognition and semantic segmentation tasks. To the best of our knowledge, all these test-time data augmentation approaches are introduced in a heuristic manner. The proposed method, by contrast, automatically generates an ensemble of TTA. It, therefore is easily utilised for other less-studied image retrieval tasks such as logo retrieval, and is useful for discovering other robust and helpful data augmentations.

In this work, we seek to learn an optimal test-time data augmentation policy through reinforcement learning. Similar approaches have been proposed for image recognition tasks to

learn the optimal train-time data augmentation, but not test-time augmentation. Cubuk et al. (2019) applied a reinforcement learning method to find the best data augmentation policy. However, their method is computationally infeasible for users with limited computational resources, as the hyper-parameter search converges only after repeatedly training a deep CNN network over 15,000 times. Alternative efficient approaches reduce the computational cost by minimising the number of training runs of the large deep learning model through the training of smaller models. For example, Ho et al. (2019) applied a Population Based Training scheme to learn a candidate schedule by training a population of k (i.e., 16) tiny models, then trained the target full size model with the candidate data augmentation schedule. Lim et al. (2019) proposed a more efficient search strategy by avoiding repeated training of child models and the target model. In contrast, we apply the same reinforcement learning based search method proposed by Cubuk et al. (2019), and find learning a TTA scheme is computationally feasible compared to learning a set of data augmentations at training time, as no backpropagation of the deep CNN model is required to learn the ensemble of TTA. We further minimise the cost by avoiding repeated forward propagation through caching. Our proposed method, therefore, is computationally efficient, yet it still able to train for in excess of 10,000 iterations in a short period of time.

2.2. Content-based Image Retrieval with Deep Features

Deep CNN features are also applied to CBIR tasks following their success in other computer vision tasks. In CBIR, deep CNN features show competitive performance compared to the hand-crafted features Tolias et al. (2015); Kalantidis et al. (2016); Tursun et al. (2019). Unlike hand-crafted features, deep features are free from heavy feature engineering and have a smaller feature size. The performance of deep CNN features in CBIR tasks is further improved by two types of approaches: fine-tuning CNNs, and applying additional processes during the feature extraction step. As the proposed approach belongs to later category, here, we mainly discuss approaches which improve the performance of deep features by applying pre/post processing during feature extraction.

Pre-processing approaches are applied to the input image before feature extraction, while post-processing approaches are applied to the extracted off-the-shelf features. Considering post-processing approaches, special pooling and attention can be applied to the extracted deep CNN features to enhance their robustness while maintaining a compact feature size. Pooling based approaches apply spatial pooling to each channel of extracted features. For examples, MAC Tolias et al. (2015) applies max pooling, while SPoC Babenko and Lempitsky (2015) applies average pooling. GeM Radenovic et al. (2018) is a generalised version of average and max pooling. R-MAC applies MAC pooling on multiple regions at various scales. Attention-based approaches apply spatial-wise and channel-wise weightings to the extracted CNN features prior to pooling. CRoW Kalantidis et al. (2016) applies spatial-wise and channel-wise weights, which are calculated from the extracted deep features. Jimenez et al. (2017) utilises class activation maps (CAM) extracted from pre-trained networks as spatial weights. Tursun

et al. (2019) also utilises CAM but uses a fine-tuned CNN trained to identify essential components in images. The proposed method is a pre-processing approach that applies multiple data augmentations to the input image before feature extraction. Other pre-processing based approaches also apply data augmentations, such as cropping Tursun et al. (2019) and scaling Tursun et al. (2021); Seddatti et al. (2017), however such approaches are heuristically defined while the data augmentations applied in our approach are learned from the data.

3. Proposed Method

In the following section, we first illustrate how to generate augmented features with a learned ensemble of test-time augmentations (TTA), and then describe how an optimal ensemble of TTA is learned.

Algorithm 1 DEEP Feature Extraction with TTA

Input: Image I , Model f , Ensemble of transformations T , Weights of transformations W

Output: Feature $\hat{\mathbf{f}}(I)$

```

1:  $F^{(T)} \leftarrow []$ 
2: for  $t_j \in T$  do
3:    $I' = t_j(I)$  ▷ Apply transformation  $t_j$  on  $I$ 
4:    $f_i = f(I', i)$  ▷ Extract features from  $i$ th layer of  $f$ 
5:    $\hat{f}_i = \text{post\_processing}(f_i)$ 
6:    $F^{(T)}.append(\hat{f}_i)$ 
7: end for
8:  $\hat{\mathbf{f}}(I) = \text{weighted\_average}(F^{(T)}, W)$ 
9: return  $\hat{\mathbf{f}}(I)$ 
```

3.1. Building a Robust Feature from an Ensemble of TTA

An augmented feature $\hat{\mathbf{f}}(I)$ for image I is generated by aggregating features extracted from transformed variants of I . This subsection describes the feature extraction process, and the procedure is also described in Algo. 1.

The features used for aggregation are extracted using the following feature extraction protocol used in the recent studies of Babenko and Lempitsky (2015); Radenović et al. (2018); Kalantidis et al. (2016). Consider $f_i(I)$ to be the extracted features from the i th layer of a CNN when I is the input image. The i th layer usually a convolutional or fully-connected layer. If the i th layer is a convolutional layer, $f_i(I)$ is a 3D tensor of width W , height H , and channels C . The extracted feature is transformed into a 1D vector by reshaping, encoding or pooling. Conventionally, a pooling process such as channel-wise max pooling (MAC) Azizpour et al. (2015) or sum pooling (SPoC) Babenko and Lempitsky (2015) is applied to $f_i(I)$ to obtain a compact feature. Further, post-processing operations such as PCA whitening and normalisation may also be applied. In this work, aggregation, PCA whitening and L2 normalisation are applied to the feature $f_i(I)$, to obtain $\hat{f}_i(I)$.

Let t_j represent the j th type of image transformation, and $T = \{t_j | 1 \leq j \leq n\}$ is an ensemble of n transformations. The

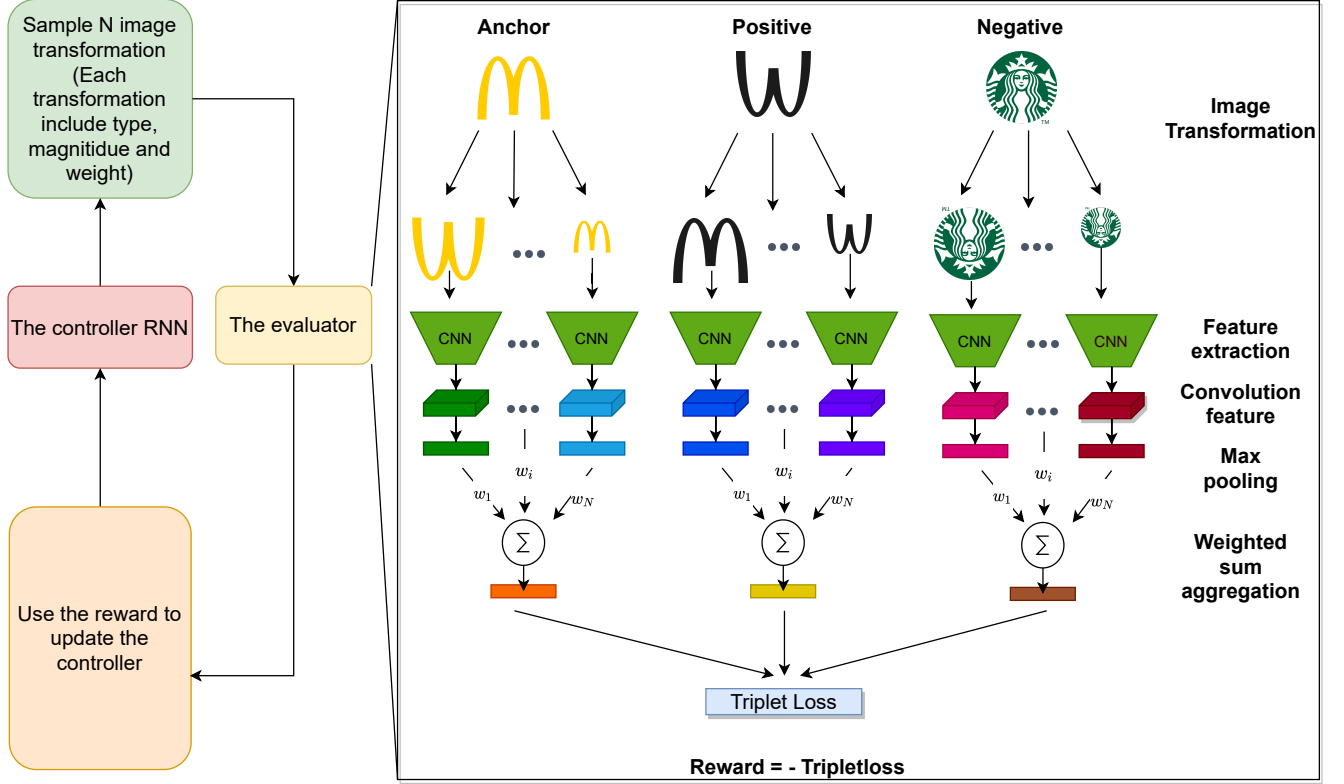


Fig. 1: The proposed scheme for searching for the optimal set of test-time data augmentations to enhance off-the-shelf CNN feature robustness for image retrieval. A controller, an RNN (for details see Fig. 2), is used to search for an ensemble of image transformations which is evaluated with a triplet network (details are given in Sec. 3.2.1). The ensemble of image transformations is applied to augment images that are sent to the triplet network for feature extraction. Extracted features are aggregated (sum aggregation), and the aggregated features is used to calculate the triplet loss whose negative value is the reward. Finally, the reward is used to update the controller.

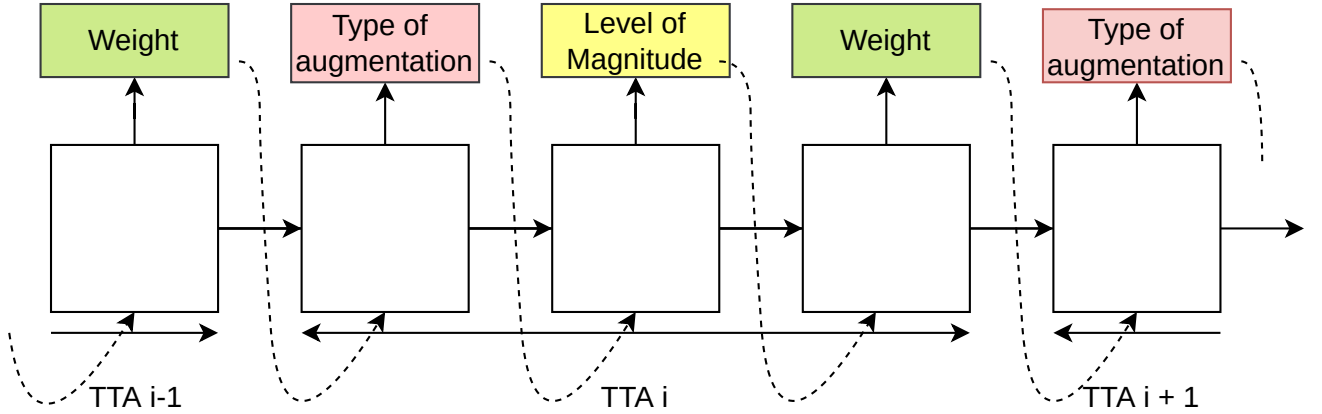


Fig. 2: The structure of the controller RNN. It is a one-layer LSTM with 256 hidden nodes and which outputs $3 \times N$ softmax predictions. It generates N TTA, and each of which is parameterised by a type, magnitude, and weight.

ensemble of features $F^{(T)}$ extracted from image I by applying the transforms T is given by,

$$F^{(T)} = \{\hat{f}_i(t_j(I)) | 1 \leq j \leq n\}. \quad (1)$$

In this work, the final augmented feature $\hat{\mathbf{f}}(I)$ is generated through a weighted sum aggregation of $F^{(T)}$,

$$\hat{\mathbf{f}}(I) = \sum F^{(T)} = \sum_{j=1}^n w_i \hat{f}_i(t_j(I)). \quad (2)$$

Finally, $\hat{\mathbf{f}}(I)$ is L2 normalised, and can be compared to other features using Euclidean distance.

In this work, the feature extraction during training and inference follows the same aforementioned protocol. In our experiments, the MAC pooling of the last activation layer of the Conv5 block of VGG16 [Simonyan and Zisserman \(2014\)](#) is used.

3.2. Learning an Ensemble of Image Transformations

In this work, finding the best ensemble of image transformations for off-the-shelf feature augmentation is formulated as a discrete search problem. Inspired from the work by Cubuk et al. (2019), we apply Reinforcement Learning (RL) to determine the optimal ensemble of TTA for the target image retrieval task. This approach finds the best policy, S , which includes n learned image transformations, and comprises the transformation operations and their corresponding magnitudes and weights. The range of magnitudes is discretised into 10 values. Weights are also discretised into 10 levels: 0 to 10, but their L1 normalised values are applied during weighted sum aggregation. To this end, if we sample N image transformations, the search space would be $(16 \times 10 \times 10)^n$. In this work, n is set to 8, as setting n too large increases the computational cost, while using too small a value of n decreases the diversity of the learned transformations which has a negative impact on performance.

A recurrent neural network (RNN) based controller is trained to sample policies, as each policy is a sequence of augmentations. The controller is a one-layer LSTM Hochreiter and Schmidhuber (1997) with 256 hidden units and $3 \times N$ softmax predictions for the N predicted transformations and their corresponding magnitudes and weights. At each step, the RNN produces a decision using a softmax classifier and sends it to the next step as an input for the next decision. In total, the controller has $3 \times N$ softmax predictions. The final sequence of decisions is the policy S , which is sent to the evaluator for evaluation. The evaluation score is used as the reward, R . The controller is updated with R . An overview of this process is given in Fig. 1, and the structure of controller is described in Fig. 2.

3.2.1. Evaluating the Learned TTA Policy

The TTA policy generated by a controller is evaluated with the evaluator module displayed in the Fig. 1. The evaluator assigns a high reward for a valid TTA policy and vice versa. A valid TTA policy should be capable of generating distinctive augmented features from off-the-shelf features extracted using a pre-trained neural network. Distinctive features for image retrieval will keep similar images close and dissimilar images distant in the feature space. To this end, we applied a triplet network Schroff et al. (2015), which is widely used for deep metric learning. As shown in the evaluator module in Fig. 1, the evaluator is a triplet network with three branches: anchor, positive and negative. Features extracted from the anchor and positive branches are should be similar, while features extracted from the anchor and negative branches should be dissimilar. These three branches will share weights and are not updated during training. The same learned transformations are applied to the anchor, positive and negative images of the triplet before sending them to the corresponding branches for feature extraction. In this work, VGG16 is the backbone network of the branches. The final augmented feature is a weighted sum of the N features from N transformed images. Augmented features are extracted for all triplets from the training dataset with a Triplet network.

The final reward, R , is given by,

$$R = -\frac{1}{k} \sum_{i=1}^k \max(\|\hat{\mathbf{f}}(I_i^a) - \hat{\mathbf{f}}(I_i^+)\|_2 - \|\hat{\mathbf{f}}(I_i^a) - \hat{\mathbf{f}}(I_i^-)\|_2 + \alpha, 0), \quad (3)$$

where k is the total number of triplets, and I_i^a, I_i^+, I_i^- is the i th triplet. α is the margin, and it is set to 0.2 as Schroff et al. (2015) recommended.

3.2.2. The Collection of Image Transformations

We create a collection of image transforms that includes the following 17 transformations: *Resize, Rotate, ShearX/Y, TranslateX/Y, AutoContrast, Invert, Equalise, Solarise, Posterise, Contrast, Colour, Brightness, Sharpness, Horizontal-flip and Contour*. It includes most of the image transformations collected by Cubuk et al. (2019) except for Cutout and Sample pairing, which are not useful for CBIR tasks. In addition, we add three new promising transformations: *Resize, Horizontal-flip and Contour*. These three additional transformations have been heuristically used as test-time augmentations in prior works. For example, Horizontal-flip is used for augmenting the test set in image classification tasks Krizhevsky et al. (2012); Simonyan and Zisserman (2014) while *Resize* is used for generating multi-scale features in landmark image retrieval Radenović et al. (2018) and trademark retrieval Tursun et al. (2021) tasks. We introduce the *Contour* (or *edge*) operation as contour based shape matching is robust to illumination changes and domain difference in image retrieval tasks Radenovic et al. (2018).

All these data augmentations are implemented with the popular Python image library, PIL¹. We use the same operation magnitude ranges suggested by Cubuk et al. (2019), except for *Rotate, Translate X/Y, Posterise and Brightness*. We increased the range of the *Rotate* operation, so it will cover upside down cases. We updated the ranges of *Translate X/Y, Posterise and Brightness* to prevent images appearing similar after the augmentation step. For example, images become black when the *Brightness* is set to zero. A detailed description of these transformations and their magnitude ranges are given in Table 1.

3.2.3. Accelerated Training via Off-line Caching

Compared to other works i.e., neural architecture search (NAS) Cubuk et al. (2019); Zoph et al. (2018), one iteration of the proposed method takes a comparatively small amount of time as the feature extraction network is fixed (i.e. it is not updated during training). However, to further speed up the process, we cache features from previous iterations such that features are extracted only once for each data transformation. We load features for each data augmentation from the hard disk in a sequential order and process aggregation operations in-place, so memory cost does not increase with the number of transformations applied. This simple approach accelerates the whole training process by a factor of 100. With a GeForce GTX 1080 graphic card, a single training iteration takes around 3 – 5 seconds on our training dataset.

¹<https://pillow.readthedocs.io/>

Table 1: List of all image transformations used in this work. The majority of the data augmentations are the same data augmentations introduced by Cubuk et al. (2019), though new operations and new settings are introduced for CBIR task. Operations shown with bold font are newly added data augmentations, while underlined operations are contain different settings. Note all these transformations are included in the PIL^a library.

id	Operation	Name Description	Range of Magnitudes
1	Resize	Resize the largest side of the image to the magnitude size with preserving the original aspect ratio. Two different ranges are applied for trademark and landmark images.	[64, 352] (trademarks), [384, 1536] (landmarks)
2	<u>Rotate</u>	Rotate the image by the rate magnitude degrees.	[-180, 162]
3-4	<u>ShearX (Y)</u>	Shear the image along the horizontal (vertical) axis by the rate magnitude.	[-0.3, 0.3]
5-6	<u>TranslateX (Y)</u>	Translate the image in the horizontal (vertical) direction by the multiplication of the magnitude with the width (height). The input image is extended by reflecting the edge of last pixels.	[-0.45, 0.36]
7	AutoContrast	Maximise the image contrast, by making the darkest pixel black and lightest pixel white.	
8	Invert	Invert the pixels of the image.	
9	Equalise	Equalise the image histogram.	
10	Solarise	Invert all pixels above a threshold value of magnitude.	[0, 256]
11	<u>Posterise</u>	Reduce the number of bits for each pixel to magnitude bits.	[1, 8]
12	Contrast	Control the contrast of the image. A magnitude=0 gives a gray image, whereas magnitude=1 gives the original image.	[0.1, 1.9]
13	Colour	Adjust the colour balance of the image, in a manner similar to the controls on a colour TV set. A magnitude=0 gives a black white image, whereas magnitude=1 gives the original image.	[0.1, 1.9]
14	<u>Brightness</u>	Adjust the brightness of the image. A magnitude=0 gives a black image, whereas magnitude=1 gives the original image.	[0.4, 1.9]
15	Sharpness	Adjust the sharpness of the image. A magnitude=0 gives a blurred image, whereas magnitude=1 gives the original image.	[0.1, 1.9]
16	Horizontal-flip	Flip the image in horizontal direction.	
17	Contour	Extract the contour of the image.	

^a python-pillow.org

3.2.4. Training the Controller

We optimise the controller with the Proximal Policy Optimisation algorithm [Schulman et al. \(2017\)](#), inspired by [Cubuk et al. \(2019\)](#); [Zoph et al. \(2018\)](#). The controller is trained with a learning rate of 10^{-4} . In total, the controller samples about 10,000 policies (the mode converges before 10,000 steps). The policy generated by the converged model is selected for inference.

4. Experiment

We tested the proposed method on both trademark and landmark image retrieval tasks, which are challenging and well-known content-based image retrieval tasks. In the following sub-sections, we present the datasets, evaluation metrics, experimental setup, and results.

4.1. Datasets

In this study, The proposed method is evaluated with two well-known CBIR tasks: trademark retrieval and landmark retrieval. Two different datasets are selected from the same domain for training and testing for each task. For example, the NPU trademark dataset [Lan et al. \(2017\)](#) is selected as the training dataset, and the METU dataset [Tursun et al. \(2017\)](#) is selected as the testing dataset for trademark image retrieval. NPU is a small dataset that includes 317 similar trademark groups and each group contains at least two similar trademarks. In total, 100,000 trademark triplets are created with these similar groups. In each triplet, the anchor and positive image are drawn from one of the 317 similar groups to obtain a similar image pair, while the negative image is randomly selected from a different group (i.e. one of the other 316 groups). Example triplets are shown in (a-b) of Fig. 3. In comparison, the METU dataset includes nearly one million trademarks. We also created a small subset of the METU dataset by selecting 10K random images from it. This subset is used for ablation studies.

Similarly, a small subset of Google Landmark Dataset [Noh et al. \(2017\)](#) is used for training, and the ROxford5k [Philbin et al. \(2007\)](#); [Radenović et al. \(2018\)](#) and the RParis6k Datasets are used [Philbin et al. \(2008\)](#); [Radenović et al. \(2018\)](#) are selected for testing in the landmark retrieval task. The revised Oxford5k dataset includes 4,993 images (includes 70 queries), and the Paris6k dataset has 6,322 images (includes 70 queries). Both datasets have three evaluation setups of different difficulty (easy, medium and hard).

We also build 100,000 landmark triplets for training. To do this, we first created 2,442 similar landmark pairs through grouping two randomly selected images from each of the most frequently appearing 2,442 unique landmarks in the Google Landmark dataset. Each landmark triplet is composed of anchor and positive images belong the same similar pair, and a negative image from a different similar pair. Example triplets are shown in (c-d) of Fig. 3.

4.2. Evaluation Metrics

We adopt the evaluation metric, *mean average precision* (MAP), shown in Equation 4, which is widely used in related



Fig. 3: Examples of triplets from the METU trademark and the Google landmark datasets. (a-b) are trademark triplets, while (c-d) are landmark triplets. Individual images in each group are, from left to right: anchor, positive and negative.

literature [Tursun et al. \(2017\)](#); [Radenović et al. \(2018\)](#). It is calculated using ranking positions obtained by sorting the image to query similarity distance in descending order. Note the MAP value is calculated using the top 100 ranking results for the METU trademark dataset, while for both Oxford5k and Paris6k datasets MAP is calculated from top 10 retrieved results.

$$MAP@K = \frac{1}{Q} \sum_{i=1}^Q \frac{1}{E_i} \sum_j^k \frac{c_j}{j}, \quad (4)$$

where Q is the number of queries, and E_i is the number of expected results of the query i . r_j is one when image with rank j is the expected image, and otherwise is zero.

4.3. Experiment Setups

Images are resized before being passed to the networks for feature extraction. All trademark images from the METU dataset are resized 224×224 , and all landmark images from Oxford5k and Paris6k datasets are resized to a maximum 1024×1024 . The aspect ratio is kept the same as the original in during the resize operation. To achieve this, padding is applied to the METU dataset, while no padding is applied for the landmark images.

All experiments were conducted on a PC with a single NVIDIA 1080 Ti graphic card, a 3.40GHz Intel Core i7-6700 CPU, and 32Gb RAM.

4.4. Results and Analysis

We selected the policy sampled by the controller after the policy converged on the training datasets. The same policy is used for our main evaluation and ablation studies. The policy learned for trademarks on the NPU dataset is: *Color*: (1, 7), *Color*: (1, 2), *Contour*: (1, 1), *Contrast*: (1, 1), *Solarise*: (1, 3), *Solarise*: (9, 1), *Solarise*: (4, 1), *Solarise*: (2, 1), and the policy learned on the sub-set of Google landmark dataset for landmark images is: *TranslateY*: (3, 2), *TranslateY*: (2, 4), *Resize*: (2, 4), *TranslateY*: (1, 4), *Resize*: (1, 3), *Resize*: (1, 3), *Resize*: (1, 3), *Resize*: (1, 1). Visualised policies with a sample image are shown in Fig. 4. Of note, the controller has learned two different policies for two different tasks.

Network Transferability We tested the learned policies with several ImageNet pre-trained networks including VGG16

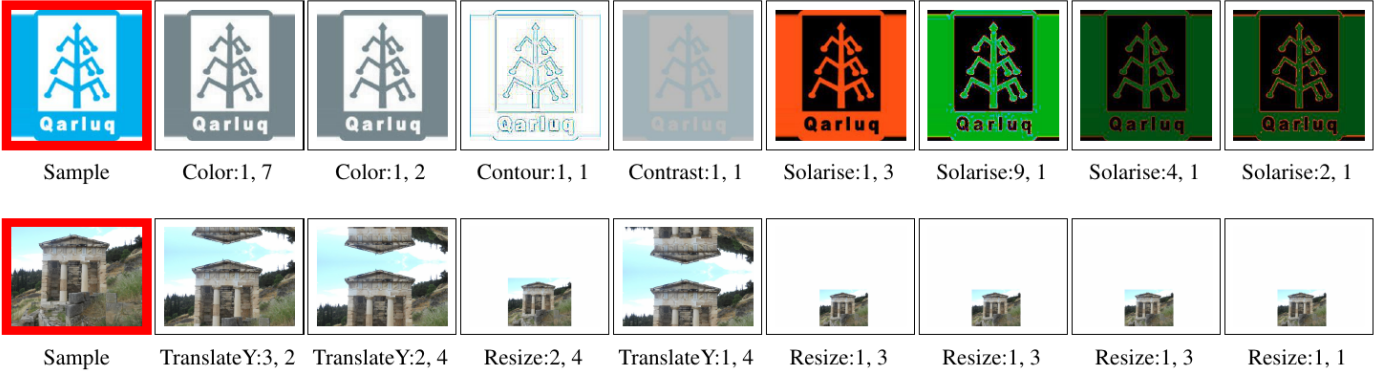


Fig. 4: Visualisation of the learned ensemble of TTA with a sample image. Under each transformed image, the applied image transformation, magnitude and weight are given. The top row shows the ensemble for trademark retrieval, while the bottom row shows the ensemble for landmark retrieval. Note that the resize operation shows only an approximate transform in consideration of the page limit and figure readability.

Simonyan and Zisserman (2014), ResNet He et al. (2015), DenseNet121 Huang et al. (2017) and AlexNet Krizhevsky et al. (2012). All pre-trained models are from TorchVision². The feature extraction layers and results are shown in Table 2. With the learned TTA, all MAP results have increased significantly compared to those without TTA. The learned TTA, therefore, has a good network transferability.

Aggregation Transferability Here, we tested the learned policy with other types of aggregation methods, namely SPoC Babenko and Lempitsky (2015), GeM Radenović et al. (2018), CRoW Kalantidis et al. (2016) and R-MAC Tolas et al. (2015). Features extracted from the last activation layer of Conv5 of VGG16 are used for implementing these aggregation methods. Hyper-parameters used in these methods are same to those in Radenović et al. (2018).

From the results shown in Tab. 3, we can see the overall MAP results of all aggregation methods are improved. This shows the learned TTA is transferable to other aggregation methods. Nevertheless, we noticed MAC pooling achieves the largest improvement compared to other aggregations. A further improvement might be achievable for other aggregations if the same type of aggregation is applied during training and testing, as is the case for MAC aggregation.

Useful Image Transformations and the Role of Weights We calculate both normal and weighted occurrence rates of all transformations in unique policies sampled during training on the trademark and landmark tasks. These results are shown in (a-b) Fig. 5. The most frequently appearing transformations also appear in the best-learned policy. For instance, in the landmark task, Resize and TranslateY operations the most frequently appearing operations. The resize operation corresponds to multi-scale operations applied in the landmark retrieval task. This finding further proves that the proposed methods learn valuable transformations. In comparison, TranslateY has not been used in any landmark retrieval studies. The TranslateY operations in the best policy direct attention to the roof region of the buildings by removing the bottom part of the building and reflecting the upper portion. This may be a result to the

roof portion of buildings having more discriminative features. On the other hand, in the trademark retrieval task, operations such as Invert, Solarise, Contrast, Color, Horizontal-flip and Contour frequently appear in the sampled policies. However, the resize and rotate operations have low occurrence rates. This is because the training data does not have scaling and rotation variance.

The difference between normal and weighted frequency shows the learned weights also contribute to the performance. For example, in the landmark retrieval task, resize operations get more weight compared to the TranslateY operations. In the trademark retrieval task, the Color operations with magnitude one get the largest weight. Note the Color operations with magnitude one only turn images into grayscale. Here, we can conclude that the learned weights enhance the contribution factor of the most important image transformation. These findings conform to the results of previous studies. For instance, multi-scaling have been widely used in landmark retrieval Radenović et al. (2018), and color-based features demonstrate poor performance compared to other shape-based features in trademark retrieval Tursun and Kalkan (2015).

The learned policy for trademark retrieval assigns more importance to the shape similarity of trademarks than their color similarity.

Network Convergence Speed On both landmark and trademark retrieval tasks, the proposed method converges after 2,000 iterations as shown in Fig. 6. In our settings, each iteration takes less than 5 seconds. The training, therefore, takes three to four hours on average.

Feature Extraction Time The proposed method processes multiple test-time data augmentations and extracts features for each type of data augmentation. If this process is done in a sequential manner this will increase the processing time by a factor of approximately N , where N data augmentations are applied. In this work, the maximum N is 8, and the CPU processing time of our method with sequential processing is on average 0.08(s) per image, which is around 10 times the baseline time of 0.008(s). However, we reduced the processing time to 0.02 (s) by parallelizing data augmentations and feature extraction.

Comparison with State-of-the-art Results We also tested

²<https://pytorch.org/docs/stable/torchvision/models.html>

Table 2: Results of off-the-shelf features from ImageNet pre-trained models with/without the learned ensemble of TTA. Results of learned image transformations are highlighted in bold if improved.

Networks	Layer	Dim	TTA	METU-10K (MAP@100)	ROxford (MAP@10)			RParis (MAP@10)		
					Easy	Medium	Hard	Easy	Medium	Hard
VGG16	Conv5	256		33.49	55.22	58.57	30.29	89.15	92.00	62.00
			✓	41.86	67.72	69.57	34.29	91.57	95.29	73.14
VGG16	Conv5	512		28.71	58.24	59.4	29.49	89.42	92.86	64.29
			✓	40.29	69.52	68.76	34.71	91.62	95.14	71.86
AlexNet	Conv5	256		28.69	44.19	41.9	13.43	83.43	85.71	46.14
			✓	38.42	52.94	52.14	21.00	91.14	92.43	69.00
ResNet50	Pool5	512		42.20	40.25	43.1	18.43	80.67	85.29	51.43
			✓	48.01	59.04	59.22	31.29	91.71	94.00	74.00
ResNet50	Pool5	2048		39.80	44.43	48.57	20.29	86.71	90.00	51.29
			✓	48.76	63.87	63.1	33.00	93.14	96.29	73.57
DenseNet121	DenseBlock4	512		38.43	38.35	41.14	11.07	85.71	87.57	52.86
			✓	45.91	63.04	59.50	23.68	93.43	95.43	74.29
DenseNet121	DenseBlock4	1024		37.31	50.31	50.12	18.62	88.14	90.29	61.14
			✓	45.16	69.68	65.48	29.29	94.57	96.71	79.29

Table 3: Results of off-the-shelf features from ImageNet pre-trained models with/without the learned ensemble of TTA. Results of learned image transformations are highlighted in bold if improved.

Dim	TTA	METU-10K (MAP@100)	ROxford (MAP@10)			RParis (MAP@10)		
			Easy	Medium	Hard	Easy	Medium	Hard
MAC		33.49	55.22	58.57	30.29	89.15	92.00	62.00
	✓	41.86	67.72	69.57	34.29	91.57	95.29	73.14
SPoC		32.99	62.23	61.38	23.36	90.00	93.00	65.57
	✓	40.13	62.46	65.90	30.71	92.43	95.29	67.86
R-MAC		38.06	69.24	64.52	27.50	92.57	94.57	74.86
	✓	44.93	68.72	66.22	30.31	92.71	95.86	72.14
GeM		35.29	63.76	64.29	30.79	91.29	94.29	75.71
	✓	43.02	69.94	71.43	34.71	91.86	95.00	73.86
CRoW		33.15	67.07	68.76	34.29	91.00	93.71	72.00
	✓	40.92	70.74	69.43	32.60	92.00	94.71	71.43

the learned TTA on the full-scale METU trademark dataset. The results are shown in Table 4. With the TTA applied off-the-shelf ResNet50/Pool4 MAC features, a MAP@100 score of 30.5 is achieved when the feature size is 512. The score decreases to 28.6 if the feature size is reduced to 256. These results outperform all previous SOTA results except for the recent method of Tursun et al. (2021). In Tursun et al. (2021), hand-crafted TTA (namely multi-scale resizing), regional attention and a modified R-MAC are applied. In comparison, we get a comparable results using only the learned TTA and MAC aggregation.

A qualitative comparison with the previous two SOTA methods (ATR MAC Tursun et al. (2019) and MR-R-SMAC w/UAR Tursun et al. (2021)) on two challenging queries is shown in Fig. 7. In both cases, the proposed method shows outstanding results compared to two SOTA methods and the proposed approach without TTA. Although, the MR-R-SMAC w/UAR method shows comparable results for the first query, it fails on

the second query. This might be caused by the rare red background color in the METU trademark dataset. However, the proposed method is still able to return good results because of the grayscale transformations applied from the learned TTA.

5. Conclusion

In this work, we applied a reinforcement learning approach to learn an ensemble of test-time data augmentations to compose robust features for image retrieval in a computationally efficient and affordable manner. The proposed method shows improvements in the performance of off-the-shelf features, and demonstrates transferability to features extracted with different networks and using different feature aggregation methods. To the best of our knowledge, little effort has been made towards automatic test-time augmentation for image retrieval. With our promising results on standard trademark and landmark datasets, we expect to attract the CV community’s attention on the po-

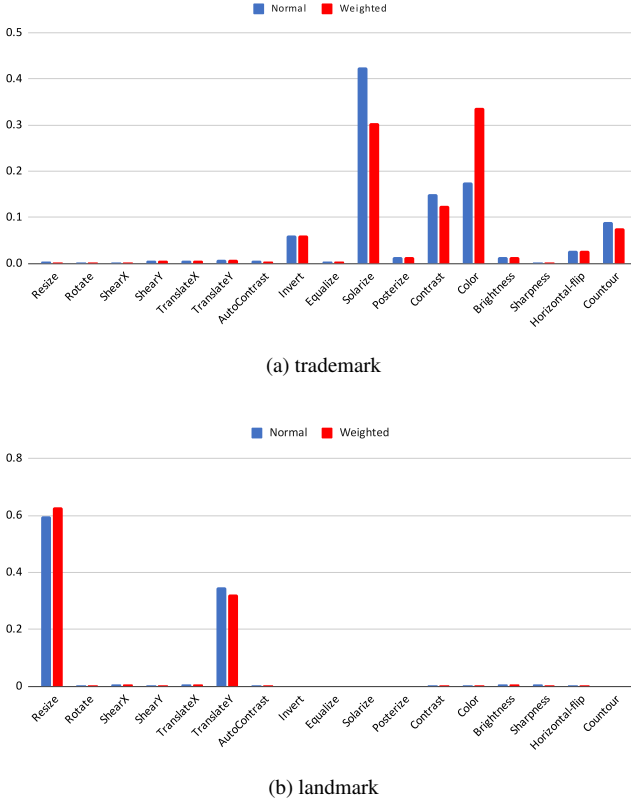


Fig. 5: The normal/weighted occurrence rate of image transformations in unique policies sampled during training on NPU trademark and Google landmark datasets.

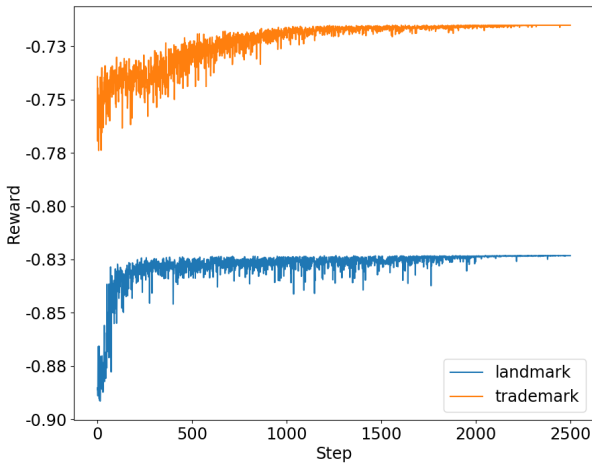


Fig. 6: The reward curves during training for landmark and trademark datasets. The model starts to converge after 2,000 steps on both tasks.

Method	DIM ↓	MAP@100 ↑
SPoC Babenko and Lempitsky (2015)	256	18.7
CRoW Kalantidis et al. (2016)	256	19.8
R-MAC Tolias et al. (2015)	256	24.8
MAC Tolias et al. (2015)	512	21.5
Jimenez Jimenez et al. (2017)	256	21.0
CAM MAC Tursun et al. (2019)	256	22.3
ATR MAC Tursun et al. (2019)	512	24.9
ATR R-MAC Tursun et al. (2019)	256	25.7
ATR CAM MAC Tursun et al. (2019)	512	25.1
MR-R-SMAC w/UAR Tursun et al. (2021)	256	31.0
Ours	512	30.5
(ResNet50/POOL4 MAC)	256	28.6

Table 4: Comparison with the previous state-of-the-art results on the METU dataset. NAR is the normalised average rank metric.

tential of boosting image retrieval performance via automatic test-time augmentation.

References

- Aker, C., Tursun, O., Kalkan, S., 2017. Analyzing deep features for trademark retrieval, in: Signal Processing and Communications Applications Conference (SIU).
- Azizpour, H., Sharif Razavian, A., Sullivan, J., Maki, A., Carlsson, S., 2015. From generic to specific deep representations for visual recognition, in: Proceedings of the IEEE conference on computer vision and pattern recognition workshops (CVPRW).
- Babenko, A., Lempitsky, V., 2015. Aggregating local deep features for image retrieval, in: Proceedings of the IEEE international conference on computer vision (ICCV).
- Ciregan, D., Meier, U., Schmidhuber, J., 2012. Multi-column deep neural networks for image classification, in: IEEE conference on computer vision and pattern recognition (CVPR).
- Cubuk, E.D., Zoph, B., Mane, D., Vasudevan, V., Le, Q.V., 2019. Autoaugment: Learning augmentation strategies from data, in: Proceedings of the IEEE conference on computer vision and pattern recognition (CVPR), pp. 113–123.
- Dai, J., Qi, H., Xiong, Y., Li, Y., Zhang, G., Hu, H., Wei, Y., 2017. Deformable convolutional networks, in: ICCV.
- Follmann, P., Bottger, T., 2018. A rotationally-invariant convolution module by feature map back-rotation, in: IEEE Winter Conference on Applications of Computer Vision (WACV).
- Gong, Y., Wang, L., Guo, R., Lazebnik, S., 2014. Multi-scale orderless pooling of deep convolutional activation features, in: European conference on computer vision (ECCV).
- He, K., Zhang, X., Ren, S., Sun, J., 2015. Deep residual learning for image recognition. arXiv preprint arXiv:1512.03385.
- Hinton, G.E., Krizhevsky, A., Wang, S.D., 2011. Transforming auto-encoders, in: International conference on artificial neural networks (ICANN).
- Ho, D., Liang, E., Chen, X., Stoica, I., Abbeel, P., 2019. Population based augmentation: Efficient learning of augmentation policy schedules, in: International Conference on Machine Learning (ICML), pp. 2731–2741.
- Hochreiter, S., Schmidhuber, J., 1997. Long short-term memory. Neural computation.
- Huang, G., Liu, Z., van der Maaten, L., Weinberger, K.Q., 2017. Densely connected convolutional networks, in: Proceedings of the IEEE Conference on Computer Vision and Pattern Recognition (CVPR).
- Jaderberg, M., Simonyan, K., Zisserman, A., et al., 2015. Spatial transformer networks, in: Advances in neural information processing systems (NeurIPS).
- Jimenez, A., Alvarez, J.M., Giro-i Nieto, X., 2017. Class-weighted convolutional features for visual instance search, in: 28th British Machine Vision Conference (BMVC).



Fig. 7: Comparison of top 10 results of our best method (ResNet50/Pool4 MAC with/without TTA) and the previous state-of-the-art methods (ATR MAC and MR-R-SMAC w/UAR) on the METU trademark dataset. For each query, the first row is the result of ATR MAC, the second row is MR-R-SMAC w/UAR, the third row is our method without TTA, and the last row is our method with TTA. Positive results are noted with a green box.

- Kalantidis, Y., Mellina, C., Osindero, S., 2016. Cross-dimensional weighting for aggregated deep convolutional features, in: European conference on computer vision (ECCV).
- Krizhevsky, A., Sutskever, I., Hinton, G.E., 2012. Imagenet classification with deep convolutional neural networks, in: Advances in neural information processing systems (NeurIPS).
- Lan, T., Feng, X., Xia, Z., Pan, S., Peng, J., 2017. Similar trademark image retrieval integrating lbp and convolutional neural network, in: International Conference on Image and Graphics (ICIGP).
- Lim, S., Kim, I., Kim, T., Kim, C., Kim, S., 2019. Fast autoaugment, in: Advances in Neural Information Processing Systems (NeurIPS).
- Marcos, D., Volpi, M., Tuia, D., 2016. Learning rotation invariant convolutional filters for texture classification, in: International Conference on Pattern Recognition (ICPR).
- Matsunaga, K., Hamada, A., Minagawa, A., Koga, H., 2017. Image classification of melanoma, nevus and seborrheic keratosis by deep neural network ensemble. arXiv preprint arXiv:1703.03108 .
- Nalepa, J., Myller, M., Kawulok, M., 2019. Training-and test-time data augmentation for hyperspectral image segmentation. IEEE Geoscience and Remote Sensing Letters 17, 292–296.
- Noh, H., Araujo, A., Sim, J., Weyand, T., Han, B., 2017. Large-scale image retrieval with attentive deep local features, in: Proceedings of the IEEE international conference on computer vision (ICCV), pp. 3456–3465.
- Perez, F., Vasconcelos, C., Avila, S., Valle, E., 2018. Data augmentation for skin lesion analysis, in: OR 2.0 Context-Aware Operating Theaters, Computer Assisted Robotic Endoscopy, Clinical Image-Based Procedures, and Skin Image Analysis. Springer, pp. 303–311.
- Philbin, J., Chum, O., Isard, M., Sivic, J., Zisserman, A., 2007. Object retrieval with large vocabularies and fast spatial matching, in: Proceedings of the IEEE Conference on Computer Vision and Pattern Recognition (CVPR).
- Philbin, J., Chum, O., Isard, M., Sivic, J., Zisserman, A., 2008. Lost in quantization: Improving particular object retrieval in large scale image databases, in: 2008 IEEE conference on computer vision and pattern recognition (CVPR), IEEE. pp. 1–8.
- Radenović, F., Iscen, A., Tolias, G., Avrithis, Y., Chum, O., 2018. Revisiting oxford and paris: Large-scale image retrieval benchmarking, in: Proceedings of the IEEE Conference on Computer Vision and Pattern Recognition, pp. 5706–5715.
- Radenovic, F., Tolias, G., Chum, O., 2018. Deep shape matching, in: Proceedings of the european conference on computer vision (eccv), pp. 751–767.
- Radenović, F., Tolias, G., Chum, O., 2018. Fine-tuning cnn image retrieval with no human annotation. IEEE transactions on pattern analysis and machine intelligence (PAMI) .
- Schroff, F., Kalenichenko, D., Philbin, J., 2015. Facenet: A unified embedding for face recognition and clustering, in: Proceedings of the IEEE conference on computer vision and pattern recognition (CVPR), pp. 815–823.
- Schulman, J., Wolski, F., Dhariwal, P., Radford, A., Klimov, O., 2017. Proximal policy optimization algorithms. arXiv preprint arXiv:1707.06347 .
- Seddati, O., Dupont, S., Mahmoudi, S., Parian, M., 2017. Towards good practices for image retrieval based on cnn features, in: Proceedings of the IEEE conference on computer vision and pattern recognition workshops (CVPRW).
- Sharif Razavian, A., Azizpour, H., Sullivan, J., Carlsson, S., 2014. Cnn features off-the-shelf: an astounding baseline for recognition, in: Proceedings of the IEEE conference on computer vision and pattern recognition workshops (CVPRW).
- Simonyan, K., Zisserman, A., 2014. Very deep convolutional networks for large-scale image recognition. arXiv preprint arXiv:1409.1556 .
- Szegedy, C., Liu, W., Jia, Y., Sermanet, P., Reed, S., Anguelov, D., Erhan, D., Vanhoucke, V., Rabinovich, A., 2015. Going deeper with convolutions, in: Proceedings of the IEEE conference on computer vision and pattern recognition (CVPR), pp. 1–9.
- Tolias, G., Sicre, R., Jégou, H., 2015. Particular object retrieval with integral max-pooling of cnn activations. arXiv preprint arXiv:1511.05879 .
- Tursun, O., Aker, C., Kalkan, S., 2017. A large-scale dataset and benchmark for similar trademark retrieval. CoRR .
- Tursun, O., Denman, S., Sivapalan, S., Sridharan, S., Fookes, C., Mau, S., 2019. Component-based attention for large-scale trademark retrieval. IEEE Transactions on Information Forensics and Security (TIFS) .
- Tursun, O., Denman, S., Sridharan, S., Fookes, C., 2021. Learning regional attention over multi-resolution deep convolutional features for trademark retrieval, in: 2021 IEEE International Conference on Image Processing (ICIP), IEEE.
- Tursun, O., Kalkan, S., 2015. Metu dataset: A big dataset for benchmarking trademark retrieval, in: 2015 14th IAPR International Conference on Machine Vision Applications (MVA), IEEE. pp. 514–517.
- Wang, G., Li, W., Aertsen, M., Deprest, J., Ourselin, S., Vercauteren, T., 2018. Test-time augmentation with uncertainty estimation for deep learning-based medical image segmentation .
- Zoph, B., Le, Q.V., 2016. Neural architecture search with reinforcement learning. arXiv preprint arXiv:1611.01578 .
- Zoph, B., Vasudevan, V., Shlens, J., Le, Q.V., 2018. Learning transferable architectures for scalable image recognition, in: Proceedings of the IEEE Conference on Computer Vision and Pattern Recognition (CVPR).